Ra and Am sorption on biotite at pH 5-9 and at varying ionic strength

Pawan Kumar*, Stellan Holgersson and Christian Ekberg
Department of Chemistry and Chemical Engineering, Division of Nuclear Chemistry
Chalmers University of Technology, Kemivägen 4, SE-41296 Göteborg, Sweden

Abstract

The sorption behavior of radionuclides ^{226}Ra and ^{241}Am onto biotite was investigated over a pH range of 5 to 9 at room temperature, using pH-buffered solutions with $NaClO_4$ concentrations varying from 0.001 to 0.1 M. The study employed potentiometric titrations, and batch sorption experiments using biotite suspensions. The results from the sorption experiment were fitted by implementing the already available thermodynamic sorption model that involves one amphoteric (2-pKa) surface complexation site and one cation exchange site.

Batch sorption experiments were conducted with ^{226}Ra and ^{241}Am at concentrations of [10^{-8}M], using crushed biotite particles (0.250-0.500 mm) at a solid-to-liquid ratio of 1:500. These experiments were carried out under three different ionic strengths of $NaClO_4$ (0.001, 0.01, and 0.1 M) and at five pH levels (5, 6, 7, 8, and 9) at room temperature (~25°C), within an inert nitrogen atmosphere ([O2_22] <1 ppm) inside a glove box for one month.

For an ionic strength of 0.001 M, the sorption coefficients (R_d -value) after one month ranged from 0.21 to 9.79 m³/kg for Ra and from 0.04 to 18.10 m³/kg for Am, across the pH range of 5 to 9. At an ionic strength of 0.01 M, the R_d -value were 0.08 to 3.79 m³/kg for Ra and 0.30 to 52.43 m³/kg for Am. At the highest ionic strength of 0.1 M, the Rd values were 0.15 to 1.80 m³/kg for Ra and 0.20 to 25.66 m³/kg for Am. The results showed that pH had a significant effect on the sorption of both ^{226}Ra and ^{241}Am. Furthermore, increasing ionic strength decreased Ra sorption but did not affect Am sorption.

To fit the sorption data, the model accounted for biotite dissolution, which was adjusted to match the final experimental results after one month. PHREEQC geochemical modeling software, coupled with an optimization routine written in Python, was used to model the sorption data. The model effectively described the sorption behavior of both radionuclides.

To determine the acidity constants (2 pKa), acidic site density (ASD), and cation exchange capacity (CEC) of biotite, titrations were performed on a biotite suspension over a pH range of approximately 3 to 11. The titration data was modeled using PHREEQC, integrated with an error minimization routine. The results indicate that the protonation/deprotonation constants, ASD and CEC of the biotite are pKa_1 = -4.9$\pm$0.1 and pKa_2 = -7.1$\pm$0.2 , $1.7 \pm 0.1 \times 10^{-5}$ mols/g and $2.6 \pm 0.4 \times 10^{-5}$ mols/g, respectively.

Keywords: biotite, radionuclides, sorption, surface complex, ion exchange, modelling

1. Introduction

In the Swedish concept for storage of ultimate waste from the nuclear power production a deep geological repository is planned in the Forsmark areas [1]. The repository will be built following the KBS-3 concept [2], [3], [1], which incorporates a multi-barrier system. According to which the spent nuclear fuel will be sealed in copper canisters. These canisters will be placed 500 meters deep in the granitic rock formation and then surrounded by bentonite clay. It is estimated that the currently operating nuclear facilities will generate around 12,000 tons of spent nuclear fuel, necessitating the placement of approximately 6,000 copper canisters in the repository (ibid.).

In the event of a breach in a copper canister, groundwater would come into contact with the spent fuel, causing it to dissolve. The dissolved radioactive material would then pass through the bentonite layer, with the surrounding host rock serving as the final barrier to prevent further radioactive migration into the biosphere [4], [5]. Therefore, understanding the radionuclide retention properties of the bedrock matrix is crucial for ensuring the repository's safe operation.

The radionuclide sorption onto granitic rock has been thoroughly examined by SKB and the Finnish company POSIVA. The outcomes are mostly presented as K_d values, or radionuclide distribution coefficients [6], [7]. However, to gain a deeper understanding of the sorption mechanisms, only limited research has modeled these condition-dependent empirical Rd-values using condition-independent surface complexation models (SCM). These models are more versatile because they can simulate the impact of factors such as groundwater composition on sorption. Since SCMs are only applicable to pure mineral phases, each mineral must be studied individually before being incorporated into a broader model. An example of this approach is the Component Additive method [8], [9] where individual mineral SCMs are combined to simulate radionuclide behavior within the complex solid phase of the rock.

The Forsmark site is predominantly composed of granodiorite, with feldspars like K-feldspar and plagioclase making up the majority of the rock. Minor amounts of mica minerals, including biotite and chlorite, are also present. Additionally, secondary minerals such as calcite and clays are found within conductive fractures, primarily acting as fracture fillers [10], [11].Biotite was selected as the initial material for study due to its potential role in radionuclide sorption.

Biotite is a mica subgroup of the phyllosilicate mineral group. Biotite, like all phyllosilicates, consists of octahedral layers containing divalent cations, mainly Fe^{2+} and Mg^{2+}, and tetrahedral layers composed of Si^{4+}, which are coordinated with oxygen or hydroxyl groups in a tetrahedral arrangement. The structural configuration of mica follows a tetrahedral-octahedral-tetrahedral (TOT) pattern, with interlayer cations of non-hydrated, K^+, linking the TOT layers together. The process of dissolving minerals can be started by exchanging the K^+ ions in the interlayer with other hydrated cations that are less firmly bonded [12].

It has been reported in the literature that biotite has a strong radionuclide sorption capacity [13], [14], [15], [16], [17]. The sorption mainly occurs through surface complexation at the edge sites or ion-exchange, primarily on the basal planes, due to biotite's layered structure. Various edge site types are assumed in the literature, including acidic (1-pKa) and/or

amphoteric (2-pKa) sites containing hydroxyl groups such as silanol and aluminol [18]. However, the Frayed Edge Sites (FES) in weathered biotite are identified as "activated" edge sites, with activation believed to occur when interlayer K^+ ions are replaced by hydrated ions. However, it remains unclear whether FES alone are responsible for the enhanced cation uptake, if they merely facilitate increased cation diffusion into the interlayer, or if they contribute to both processes [19]. Conversely, hydroxyl edge sites have been considered as ion exchange sites in certain modeling studies [20], [17], [21].

A recent literature review on surface complexation models (SCM) for biotite and other minerals [22] identified the sorption isotherm as the most commonly used experimental method. In this approach, pH was held constant while the concentration of the sorbing element was varied, often using relatively high concentrations of radioactive elements. However, to prevent surface characteristics from being altered by radionuclide adsorption, IUPAC recommends staying well below the tracer concentration (10^{-6} M) when applying SCM to experimental data. For developing a reliable model, SCM studies should ideally explore a broad range of solution conditions, including pH, ionic strength, and temperature [23].

The analysis also highlighted the limited availability of datasets with systematic variations across multiple solution conditions [22]. One study investigated the impact of varying ionic strength while maintaining a constant pH for alkaline earth metals [21] Another study varied the concentration of Ba(II) while keeping ionic strength and pH fixed [24] . In both studies, a three-site ion exchange model was applied to the data [21] [24]. In a separate study [25], Ra sorption was examined using four different groundwater simulants with varying salinity levels at a constant pH. The results were modeled using a multi-site surface complexation approach, incorporating one surface complexation site (one strong and one weak) and one ion-exchange site (the FES site).

Additionally, only two studies on Eu(III) sorption onto biotite accounted for variations in both pH and ionic strength. These studies used either a combination of one surface complexation site and one ion exchange site [26] or a single ion exchange site [15].

In conclusion, the SCMs reported for biotite show considerable inconsistency in terms of employed solution condition, which presents challenges for those seeking a reliable sorption model applicable to diverse water conditions.

Therefore, the objectives of this study are as follows: 1) Conduct separate experiments to characterize biotite in terms of specific surface area, cation exchange capacity, acidic site density, and surface acidity; 2) Conduct sorption experiments using biotite and a few representative elements and oxidation states, in this case Ra and Am, at concentrations well below tracer levels (10^{-8} M), with a systematic variation of pH (5-9) and ionic strength (0.001,0.01, and 0.1 M) at room temperature. 3) To use the PHREEQC geochemical modeling software in conjunction with an optimization procedure for PYTHON programming to derive the SCM constants in order to model the measured Rd values.

2. Material and methods

2.1 Biotite sample preparation and its specific surface area measurement

The biotite sample used for the present study was obtained from Risör, Norway. The composition is $K_{1.05}(Mg_{0.70}Mn_{0.06}Ti_{0.18}Fe(II)_{1.81}Fe(III)_{0.25})Al_{1.28}Si_{2.62}O_{10}(OH)_2$, with the specimen's purity determined to be over 99% in the same study [27]. The density of the biotite was previously reported as 3.10 kg/m³ [28].

Due to the difficulty of crushing the mineral using a mortar and pestle, a steel-bladed blender (M20, IKA) was employed. The resulting crushed mineral was subsequently sieved into two particle size fractions using a sieve shaker (AS200, Retsch) equipped with stainless steel test sieves (200mm, ISO3310-1, Retsch). The 0.25-0.5 mm fraction was predominantly employed for batch sorption experiments, whereas the 0.063-0.125 mm fraction was designated for acidic site density measurements. The sieving process involved shaking at high amplitude for 20 to 30 minutes, followed by shaking at a lower amplitude for one hour. To remove ultrafine particles, 95% ethanol was used to wash the crushed biotite several times. Once the coarse particles settled, the clarity of the ethanol supernatant confirmed the successful removal of ultrafine particles. After drying the samples in a vacuum chamber for several days, biotite samples were collected in triplicate in order to measure its specific surface area (SSA). SSA for both size fractions were determined using a Kr gas adsorption apparatus (ASAP2020, Micromeritics) and analyzed via the BET isotherm method [29].

2.2 Mineral Characterization

Biotite specimens were previously characterized in terms of specific surface area (SSA), acidic site density (ASD), and cation-exchange capacity (CEC) (Kumar et al., submitted article). The experimentally obtained SSA, ASD, and CEC were determined to be 0.47 $\pm$0.01 m^2/g, 3.3 $\pm$ 0.6 $\times 10^{-6}$ mol/g and 1.0 $\pm$ 0.1 $\times 10^{-5}$ mol/g, respectively.

2.3 Biotite conditioning for batch sorption experiments

Before conducting the titration and batch sorption experiment, the biotite was first converted to monocationic form (Na^+-form). This was done by adding 5 ml of $NaClO_4$ (Merck, 98%) solution 0.1 M, 0.01 M, and 0.001 M ionic strength with 0.01 g of biotite in 10 ml polypropylene tubes. The samples were conditioned for 1.5 months, during which the electrolyte solutions were changed three times. After each conditioning phase, the exchangeable cations in the solutions were analyzed using an ICP-OES (Thermo iCAP Pro XP Duo). The instrument was calibrated with Na, K, Ca, and Mg standard solutions before each analysis.

2.4 Batch sorption experiments

The sorption of ^{226}Ra and ^{241}Am on Na-converted biotite was assessed using $NaClO_4$ (Merck, 98%) electrolyte solutions at concentrations of 0.001 M and 0.01 M. To buffer these solutions, 1,4-Diethylpiperazine (DEPP, Alfa Aesar, 98%) was used for pH 5 and 9, 2-(N-Morpholino)ethanesulfonic acid (MES, Sigma-Aldrich, 99%) for pH 7, and 1,4-Piperazine-bis-(propanesulfonic acid) (PIPPS, Merck, 98%) for pH 8. These organic buffers were selected due to their resistance to forming metal complexes, making them suitable for this type of study [30].

A glass electrode and pH meter (pHC3006-9, PHM240, Radiometer) were used to measure pH, with adjustments made using aliquots of 0.1 M NaOH or $HClO_4$. Buffer concentrations were set at 5 mM for the 0.1 M and 0.01 M $NaClO_4$ solutions, and 0.5 mM for the 0.001 M solution. To achieve concentrations of less than 10^{-8} M for both elements, the solutions were spiked with a mixture of acidic ^{226}Ra ($RaCl_2$ in 0.0091 M HCl) and ^{241}Am ($RaCl_3$ in 0.5 M HCl). All mixtures contained 10 µg/mL of carrier (Eckert & Ziegler). After spiking, the pH was readjusted using 0.1 M NaOH or $HClO_4$.

The fifteen spiked buffered solutions, covering five pH levels and three ionic strengths, were left to degas for several days in the glovebox antechamber. For the batch experiments, 0.1 g of Na-converted biotite was added to 10 ml polypropylene centrifuge tubes (Oak Ridge type 3119-0010, Thermo Scientific), which was pre-washed with acid. The samples were then centrifuged at 45,000g (Avanti J26S XP, Beckman Coulter). After approximately one month of equilibration in 5 ml of 0.001 M, 0.01 M, or 0.1 M neutral $NaClO_4$ solutions, the supernatants were removed. The tubes were subsequently transferred to a glovebox ($[O_2]$ <1 ppm, UNILab, MBraun) to minimize carbonate complex formation.

In each sample, 5 mL of the radioactive pH-buffered electrolyte solution was added to maintain a 1:50 solid-to-liquid ratio. In total, 45 samples were prepared in triplicate. Additionally, 15 blank samples were prepared to evaluate radionuclide sorption onto the tube walls. Two acidified reference samples were made for each radioactive solution, in order to determine the average reference radioactivity concentration at each pH.

The sorption experiment was conducted over approximately one month at a temperature of 22-25°C. Samples were collected on days 4, 8, 14, and 30. Prior to every sample, the tubes were centrifuged for 30 minutes at 45000g. An aliquot of 0.1 ml (2% of the total volume) was collected from the supernatant added with 0.4 ml of 0.1 M HCl solution, with the exception of the final sample, where 0.5 ml was taken without any acid addition. Using an HPGe detector (GEM23195 detector, 2002C preamp, DSA2000 MCA, GammaAnalyst sample changer, and Genie2000 v.3.4.1 software, Canberra/Mirion), the gamma activity of the radionuclides in the aqueous phase was monitored for three hours.

The wall sorption-corrected distribution coefficient R_d (m^3/kg) on biotite for radioactivity-based radionuclides was determined using the subsequent two formulas, which were derived from a deduction presented in [31]:

$$R_d = \left(\frac{\bar{C}\cdot V_{ref}\cdot V_{out,n}}{A_{out,n}} - \left(V_0 - \sum_{i=1}^{n-1} V_{out,i}\right) - L_d - \frac{V_{out,n}\cdot\sum_{i=1}^{n-1} A_{out,1}}{A_{out,n}}\right)\cdot\frac{1}{m} \qquad \text{(Eq.1)}$$

In (Eq.4), Vref (L) is the volume of the radioactive solution added initially, Vout,n (L) and Aout,n (cpm) are the volume and measured activity of sample n of the one to n successive samples, and $\bar{C}$(cpm/L) is the average measured reference concentration obtained from the acidic references. The batch's initial liquid volume, or V0(L), comprises Vref and any leftover liquid from the preconditioning. The mass of the material in the sorption experiment is represented by m(g), and the factor correcting for wall sorption is Ld (L), which is measured in a separate blank series of batch tests. The two summation terms in (Eq.1) are derived from an overall mass balance and serve to offset the radioactivity and volumes removed in the subsequent samplings.

Essentially the same formula is used to determine the wall sorption factor $L_{d.}$ however, since the mass involved in wall sorption is unknown, the wall sorption factor L_d (m^3) is a volume and can be evaluate as:

$$R_{d,wall}\cdot m_{wall} = \left(\frac{\bar{C}\cdot V_{ref}\cdot V_{out,n}}{A_{out,n}} - \left(V_0 - \sum_{i=1}^{n-1} V_{out,i}\right) - \frac{V_{out,n}\cdot\sum_{i=1}^{n-1} A_{out,1}}{A_{out,n}}\right) \equiv L_d \qquad \text{(Eq.2)}$$

2.5 Modelling Methods

Thermodynamic Sorption Models (TSMs), also known as Surface Complexation Models (SCMs), are complex and require multiple datasets depending on the model's complexity. Some datasets can be obtained through experiments such as cation exchange capacity (CEC), tritium exchange experiments and Brunauer-Emmett-Teller (BET) analysis. However, the remaining parameters are generally determined by fitting the titration and sorption experimental data. The data obtained from titration provides information on key parameters such as mineral's acidity constants and surface site density. On the other hand, sorption data provides information on the reaction constants occurring on the surface site.

In order to gather this information, a conceptual model of biotite, shown in Fig.1, was employed for the modeling of the sorption and titration data.

The structure of biotite and the evidence from sorption data in the literature support this conceptual model, which states that in order to explain the estimated sorption data, there should be at least one cation exchange site (X) and one acidic or amphoteric surface complexation site ($\equiv SO^-$) [22]. The exchange sites exist on the basal planes and the surface complexation sites are present on the edge of the biotite structure as shown in Fig. 1.

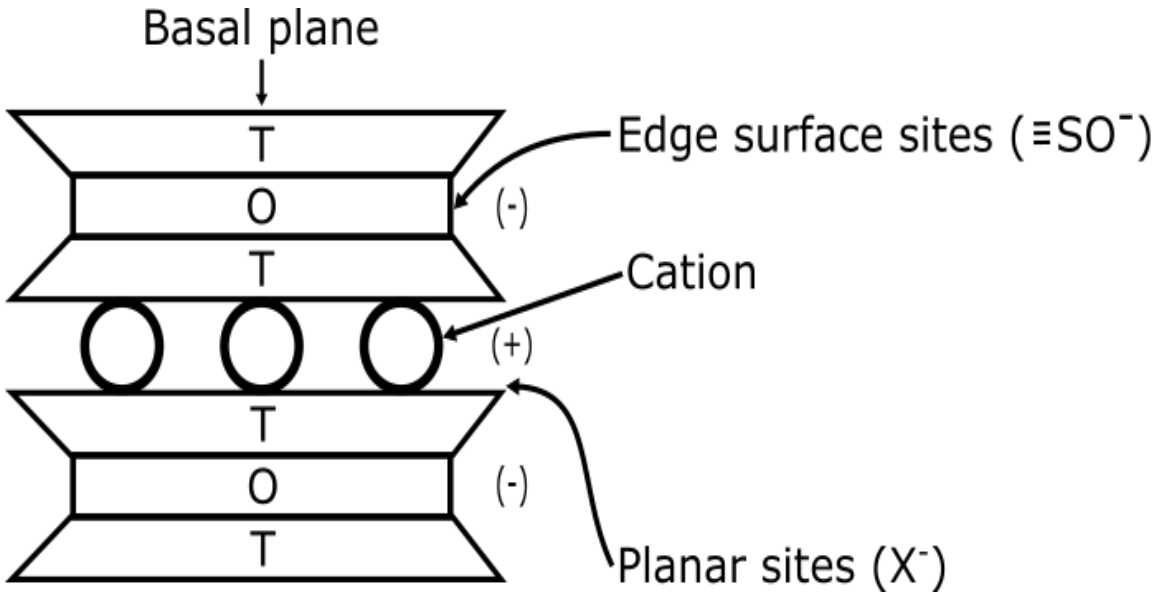

Figure.1. Conceptual model of biotite

Typically, the exchange sites are created by the isomorphic substitution of lattice elements. This type of sorption mechanism is generally not affected by pH, except at low pH levels and the uptake of radionuclide governed by the permanently charged planar sites [32] [33]. A general structure of a cation exchange reaction in which a metal M of valency Z_M exchanging with A of valency N_a on the mineral surface (X) can be written as:

$$N_aA - X + Z_aM \leftrightarrow Z_aM - X + N_aA \quad \text{(Eq.3)}$$

The selectivity co-efficient K_c defined for these reactions based on Gaines-Thomas convention [1] can be written as:

$${}^{M}_{A}Kc = \frac{B_M^{Z_a}\,\Upsilon^{A}[A]^{N_a}}{B_A^{N_a}\,\Upsilon^{M}[M]^{Z_a}} \quad \text{(Eq.4)}$$

Where, [A]and [M] is the initial electrolyte and tracer concentration(mol/L); Υ^{A} and $\Upsilon^{M}$is the activity co-efficient of the cations present in the solution determined from Davies equation (L/mol), respectively; and B_A and B_M are the equivalent fraction occupancies of A (or M) sorbed per unit mass divided by CEC (eq/kg).

However, the sorption due to surface complexation is generally affected by the protonation and deprotonation of amphoteric surface hydroxyl groups (≡ SOH). These groups are located as a broken bonds and edge sites [34] [35] [36] on the mineral surface and are mainly influenced by changes in pH values.

The initial objective was to find out which speciation of metal is most suitable for surface reactions in the experimental pH range. This information was used as a reference to select an appropriate surface chemical reaction. Thus, for non-hydrolyzed and hydrolyzed metal M with valency n on the amphoteric surface site in the pH range where metal M is present as a free aqueous species, the general sorption reaction can be stated as follows:

$$\equiv \mathrm{SOH} + \mathrm{M^n} = \equiv \mathrm{SOM^{(n-1)}} + \mathrm{H^+} \quad \text{(Eq.5)}$$

$$\equiv \mathrm{SOH} + \mathrm{M^n} + \mathrm{zH_2O} = \equiv \mathrm{SOM(OH)_z^{(n-z)}} + \mathrm{zH^+} \quad \text{(Eq.6)}$$

The surface complexation constants for these reaction without considering the electrostatic effect can be written as:

$$\mathrm{K_{M^n}} = \frac{[\equiv \mathrm{SOM^{(n-1)}}]\{\mathrm{H^+}\}}{[\equiv \mathrm{SOH}]\{\mathrm{M^n}\}} \quad \text{(Eq.7)}$$

$$\mathrm{K_{M^n}} = \frac{[\equiv \mathrm{SOM(OH)_z^{(n-z)}}]\{\mathrm{H^+}\}}{[\equiv \mathrm{SOH}]\{\mathrm{M^n}\}} \quad \text{(Eq.8)}$$

The titration data was modelled by including the following reactions:

$$NaX + H^+ \rightleftharpoons HX + Na^+ \quad \text{(R.1)}$$

$$\equiv SOH \rightleftharpoons \equiv SlO^- + H^+ \quad \text{(R.2)}$$

$$\equiv SOH_2 \rightleftharpoons \equiv SOH + H^+ \quad \text{(R.3)}$$

$$\equiv SO^- + Na^+ \rightleftharpoons \equiv SONa \quad \text{(R.4)}$$

$$\equiv SOH + Na^+ \rightleftharpoons SOHNa^+ \quad \text{(R. 5)}$$

Each of the following reactions is taken into consideration, ion-exchange between protons and the electrolyte's cation on basal planes (R.1); deprotonation of the edge surface (R.2 and 3); and a strong (R.4) and weak (R.5) surface complex with the cation, in this case from the electrolyte. The corresponding selectivity coefficient for ion exchange K_{NaX} is defined by

$$\mathrm{K}_{NaX} = \frac{[HX]\{Na^+\}}{[NaX]\{H^+\}} \quad \text{(Eq. 9)}$$

The surface protonation constant K_{a1} and K_{a2} for reaction R.2 and R.3 can be defined as:

$$\mathrm{K_{a1}} = \frac{[\equiv \mathrm{SOH}]\{\mathrm{H^+}\}}{[\equiv \mathrm{SOH_2}]} \quad \text{(Eq. 10)}$$

$$\mathrm{K_{a2}} = \frac{[\equiv \mathrm{SO^-}]\{\mathrm{H^+}\}}{[\equiv \mathrm{SOH}]} \quad \text{(Eq. 11)}$$

The surface complexation constants for Na^+ sorption reactions (R.4) and (R.5) are

$$\mathrm{K}_{SONa} = \frac{[\equiv \mathrm{SONa}]}{[\equiv \mathrm{SOH}]\{Na^+\}} \quad \text{(Eq. 12)}$$

$$K_{SOHNa} = \frac{[\equiv SOHNa^+]}{[\equiv SOH]\{Na^+\}} \quad \text{(Eq. 13)}$$

where the symbol [] indicates that the concentration is given in units of mol/L.

A non-electrostatic model was implemented to fit the distribution coefficients (R_d – values). The parameters such as site density, CEC, selectivity co-efficient, proteolysis constants, and Na^+ surface complexation constant were fixed, as shown in Table 1. The constant for the assumed reactions is the optimized parameters. It is important to note that PHREEQC treats these values as valid at zero ionic strength and adjusts the activity coefficients for all dissolved species according to the specified ionic strength. Additionally, the formation of hydroxide complexes Ra and Am had to be considered in the modeling. The incorporated hydroxide complexes for Ra and Am are listed in Table 2 below.

Table 1: Thermodynamic data of aqueous hydroxide complexes of Ra and Am used in sorption modeling for zero ionic strenght.

Reaction	**log_β**
$\mathbf{Ra^{2+} + H_2O = Ra(OH)^+ + H^+}$	0.51[a]
$\mathbf{Am^{3+} + H_2O = Am(OH)^{2+} + H^+}$	6.8[b]
$\mathbf{Am^{3+} + 2H_2O = Am(OH)_2^+ + 2H^+}$	12.9[b]
$\mathbf{Am^{3+} + 3H_2O = Am(OH)_3^0 + 3H^+}$	15.8[b]

[a]PHREEQC database ThermoChimi, [b] [37]

The literature did not provide a solubility product for biotite. Therefore, annite, an end member of the same mica solid solution series as biotite, was used as a substitute and kept in equilibrium with the solution to simulate any dissolution effects that might have occurred from biotite. The sorption data were modeled using the MINTEQ thermodynamic database integrated with PHREEQC.

The model was implemented by combining the PHREEQC version 3 geochemical modeling software [38] with the PYTHON optimization programming routine through a specialized code created by [39] named Iphreeqc.Com. This code, known as Iphreeqc, is a Microsoft COM (component object model) version of PHREEQC that enables seamless communication and data transfer between PHREEQC and other programming languages and softwares such as MATLAB, PYTHON, and Visual Basic

3. Results and Discussion

3.1. Conditioning results

After conditioning of biotite with 0.1 M, 0.01 M, and 0.001 M $NaClO_4$ for use in titration and sorption experiments, the K^+ amount was steadily decreased in the solution, giving a biotite that was 80% converted from K to Na form for 0.1 M and 0.01 M. However, in the case of 0.001 M $NaClO_4$, the conversion was only 31%.

3.2. Titration results

The optimized reaction constants are in Table 2. The complete explanation about the titration outcomes has been provided in our previous work (kumar et al.,2024 submitted article).

Table 2. Optimized reaction coefficients/constants in 0.01 M $NaClO_4$ for biotite with optimized Cation Exchange Capacity and Acidic Site Density.

Surface complexation reactions	**Constants (log_K)**
$\equiv \mathbf{SOH_2} \rightleftharpoons \equiv \mathbf{SOH} + \mathbf{H^+}$	-4.9 ± 0.1
$\equiv \mathbf{SOH} \rightleftharpoons \equiv \mathbf{SO^-} + \mathbf{H^+}$	-7.1 ± 0.2
$\equiv \mathbf{SOH} + \mathbf{Na^+} \rightleftharpoons \equiv \mathbf{SONa} + \mathbf{H^+}$	1.6 ± 0.1
$\equiv \mathbf{SOH} + \mathbf{Na^+} \rightleftharpoons \equiv \mathbf{SOHNa^+}$	0.5 ± 0.1
Cation exchange reaction	**Coefficient (log_K)**
$\mathbf{Na - X} + \mathbf{H^+} \rightleftharpoons \mathbf{H - X} + \mathbf{Na^+}$	3.0 ± 0.2
Total site capacities	**Site densities (mol/g)**
Acidic Site density (optimized)	$1.7 \pm 0.1 \times 10^{-5}$
Cation Exchange Capacity (optimized)	$2.6 \pm 0.4 \times 10^{-5}$

3.3. Batch sorption results

3.3.1. Results for Ra sorption on biotite

Figure 2 presents the time-dependent results of Ra(II) sorption on biotite in a 0.001 M $NaClO_4$ solution, exhibiting behavior similar to Ba(II) as reported in our earlier study (Kumar et al., 2024, submitted article). Like Ba(II), the Ra(II) sorption gradually increased over the first 15 days, followed by an apparent equilibrium. A complete set of time-dependent apparent R_d -values for Ra sorption on biotite is provided in Table 1, 2, 3 of Appendix A.

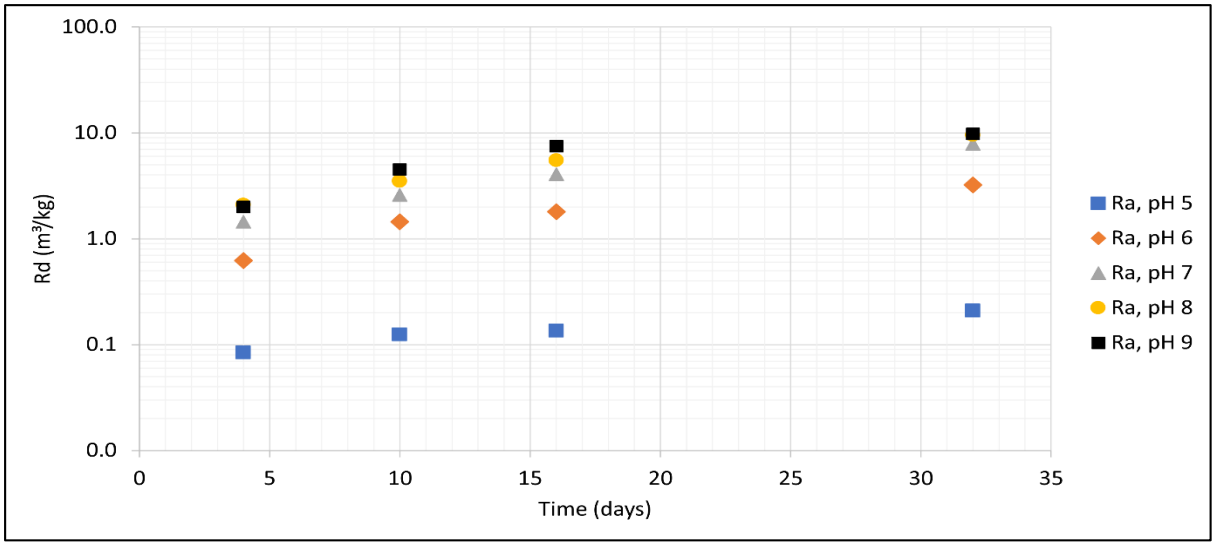

Figure 2. Measured R_d values for Ra(II) sorption onto biotite in 0.001 M $NaClO_4$ versus time.

Figure 3 presents both the experimental and modeling results for Ra sorption onto biotite as a function of pH (ranging from 5 to 9) and ionic strength (0.001M, 0.01M, and 0.1M). The findings demonstrate that both pH and ionic strength significantly influence Ra sorption. Between pH 5 and pH 8, R_d-values steadily increase at ionic strengths of 0.01M and 0.1M. A sharp rise in Ra sorption is observed between pH 8 and pH 9, likely due to the formation of barium hydroxyl species, Fig. 3. These results are consistent with our previous work on Cs, Ba,

Co, and Eu sorption onto biotite (Kumar et al., 2024, submitted article) which supports the conclusion that Ra behaves analogously to Ba, with both exhibiting similar sorption patterns.

However, a slight discrepancy was observed between the Rd values of these two alkaline earth metals: across all ionic strengths and pH levels, Ra sorption on biotite was consistently higher than that of Ba. Similar findings were reported by [21] in their study on the sorption of alkaline earth metals onto biotite, where Ra exhibited higher Rd values compared to Ba. However, their macroscopic study did not offer an explanation for the difference in Rd values between Ra and Ba. The only notable factor is that Ra has a lower hydration energy, and a larger ionic radius (152 Å) compared to Ba (135 Å) [40], which likely accounts for Ra's higher sorption relative to Ba.

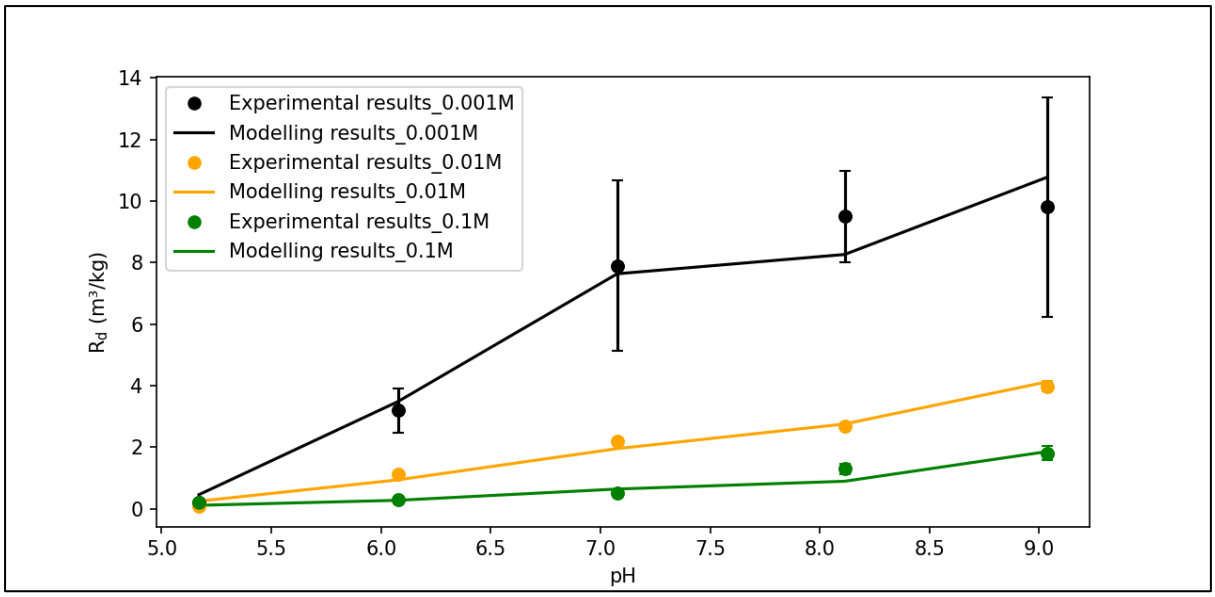

Figure 3. Experimental (points) and Modelling (line) for Ra sorption on biotite in 0.001 M, 0.01 M, and 0.1 M $NaClO_4$ solutions.

As illustrated in Fig. 4 (a, b, and c), the radium sorption data was modeled using two cation exchange surface species (RaX_2 and RaOHX) and three surface complexes ($\equiv SORa^+$, $\equiv SORaOH$, and $\equiv SOHRa^{2+}$) similar to the approach used for Ba in our previous work (Kumar et al., 2024). Although the $\equiv SOHRa^{2+}$ surface complex was initially part of the model, it was later removed as it did not improve the fit. The model results indicate that at a background electrolyte concentration of 0.001 M from pH 5 to 9, Ra sorption is primarily governed by ion exchange (RaX_2) from pH 5 to 9, with some contribution from the $\equiv SORa^+$ surface complex. However, at higher pH levels (8 to 9), both RaOHX and $\equiv SORaOH$ surface species also appear to play a role in Ra sorption.

Additionally, the modeling indicates that as the ionic strength increases from 0.001 M to 0.1 M, surface complexation becomes the dominant sorption mechanism, as depicted in Fig. 4 (a, b, c). The relevant reactions and their constants are provided in Table 3.

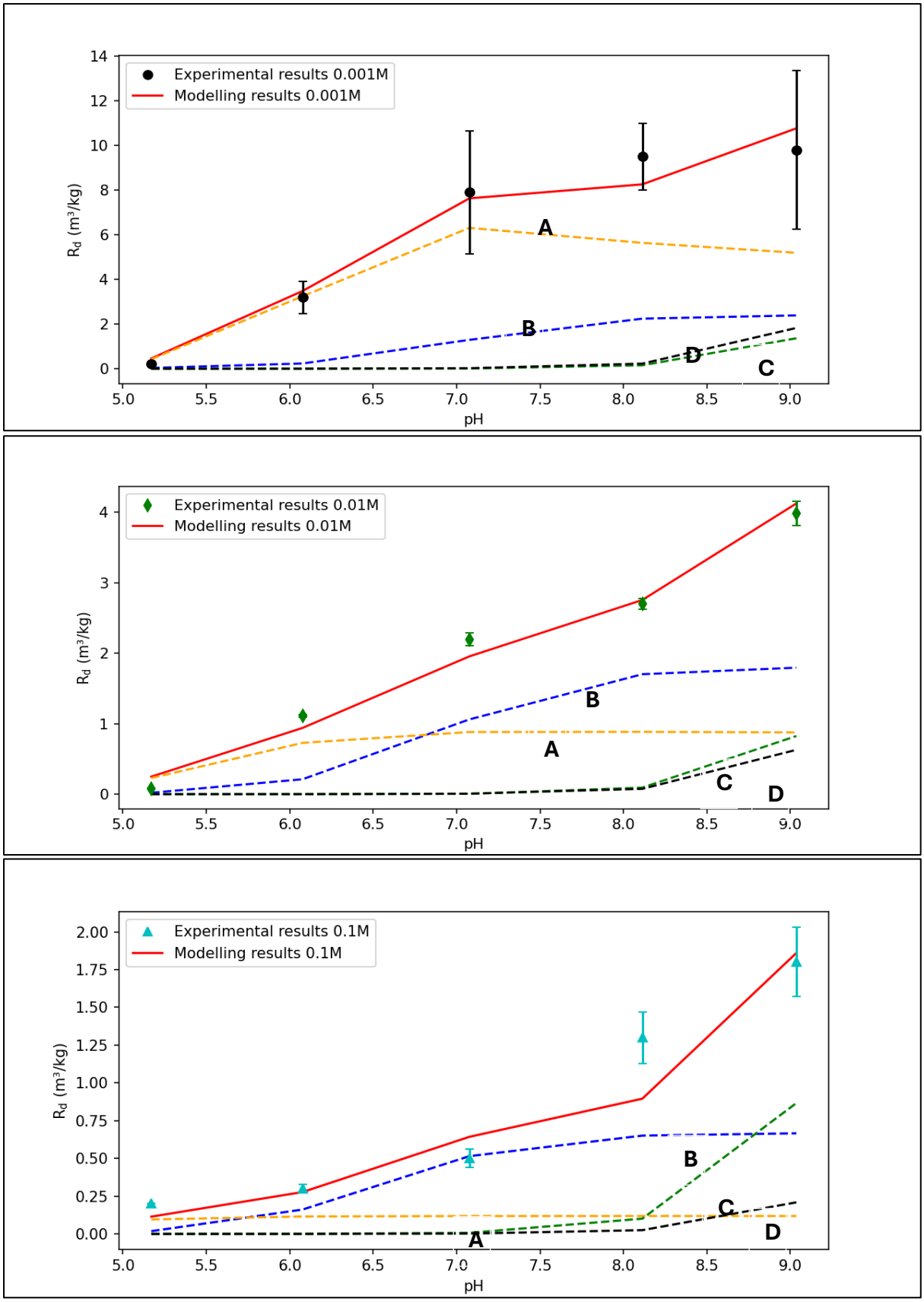

Figure 4. Experimental (symbol) and modelling (continuous line) results for Ra sorption onto biotite in (a) 0.001 M, (b) 0.01 M and (c) 0.1 M $NaClO_4$ solution at 25 °C. The contribution of different Ra(II) species in its sorption is represented by different curves:(A: Yellow line) RaX_2; (B: Blue line) ≡$SORa^+$; (C: Green line)) ≡SORaOH; (D: Black line) XRaOH

Table 3: Surface complexation and cation exchange reactions and their associated constants at zero ionic strength (log_k°) for Ra. Selectivity coefficients are for the specified ionic strength

Reactions		**log k° (25 °C)**	
$\equiv SO^- + Ra^{2+} \leftrightarrow \equiv SORa^+$		5.4 ± 0.2	
$\equiv SO^- + Ra(OH)^+ \leftrightarrow \equiv SORaOH$		9.4 ±0.5	
$\equiv SOH + Ra^{2+} \leftrightarrow \equiv SOHRa^{2+}$		Not significant*	
$NaX + RaOH^+ \leftrightarrow RaOHX + Na^+$		7.1 ±0.6	
Reaction/Ionic Strength at 25 °C	**log k (0.001 M)**	**log k (0.01 M)**	**log k (0.1 M)**
$Ra^{2+} + 2RaX \leftrightarrow RaX_2 + 2Na^+$	-0.1	1.0	2.4

*Inclusion of this species gave no improvement of error sum

3.3.2 Results for Am sorption onto biotite

Figure 5 presents the time-dependent results for americium (Am) sorption onto biotite. It was observed that Am(III) sorption stabilizes after 15 days, reaching equilibrium around day 30, except at the lowest pH of 5, where a slight decrease in Rd values is likely due to biotite dissolution. A complete set of time-dependent apparent R_d values for Am sorption onto biotite is provided in Tables 4, 5, 6 of Appendix A.

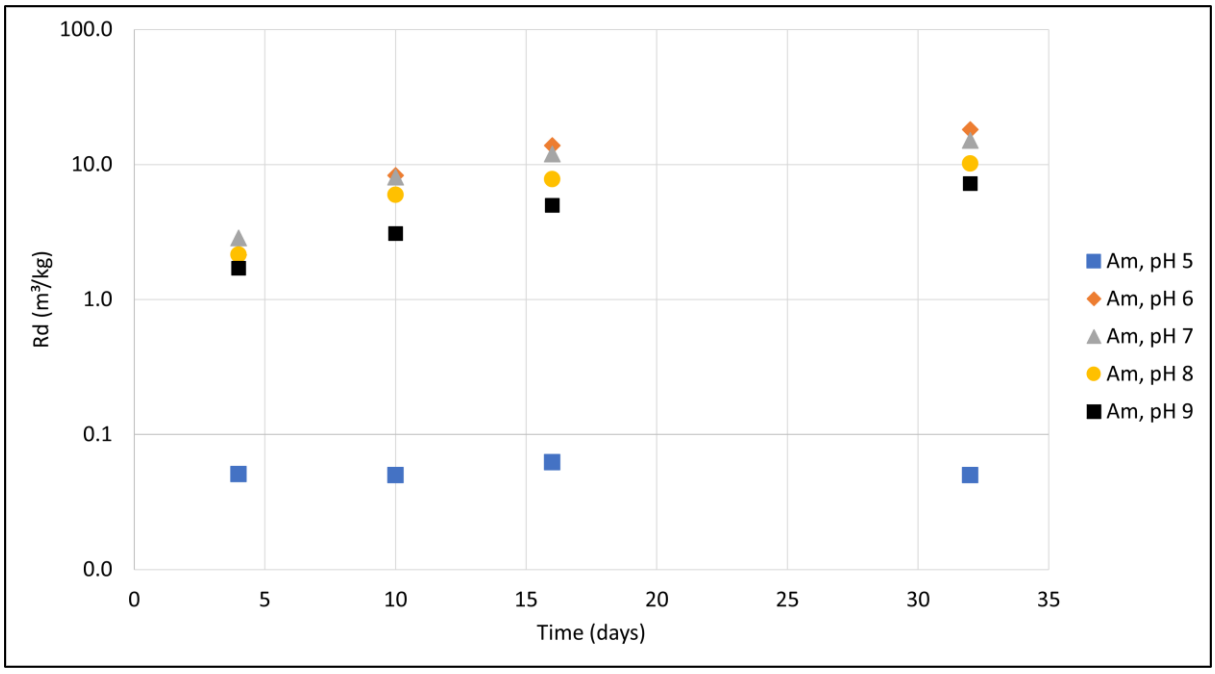

Figure 5. Measured R_d values for Am(III) sorption onto biotite in 0.001 M $NaClO_4$ versus time.

The experimental and modeling results for Am(III), shown in Fig. 6, indicate that americium behaves similarly to europium as observed in our previous study on Cs, Ba, Co, and Eu sorption onto biotite (Kumar et al 2024, submitted article). This can be due their comparable electronic configurations (Am: [Rn] $5f^7$ $7s^2$ and Eu: [Xe] $4f^7$ $6s^2$) and similar ionic radii (Am^{3+} = 98 nm, Eu^{3+} = 94.7 nm). Like Eu, the experimental results suggest that Am sorption was found to be highly pH-dependent, with no significant influence of ionic strength Fig. 6. The data shows that across all ionic strengths (0.001 M, 0.01 M, and 0.1 M), Am sorption increased sharply between pH 5 and 6, followed by a gradual decrease as pH rose to 9, likely due to the formation of aqueous hydroxide complexes.

Additionally, the experimental results indicate that the R_d values for Am are roughly 2.5 times higher (R_d = 52.3 m^3/kg) than those for Eu (18.5 m^3/kg) (Kumar et al., 2024, submitted article) across all pH levels. Similarly, in another study [41] on Am sorption onto biotite, the reported Rd value was comparable to this work around 10-30 m^3/kg at pH 6-7.

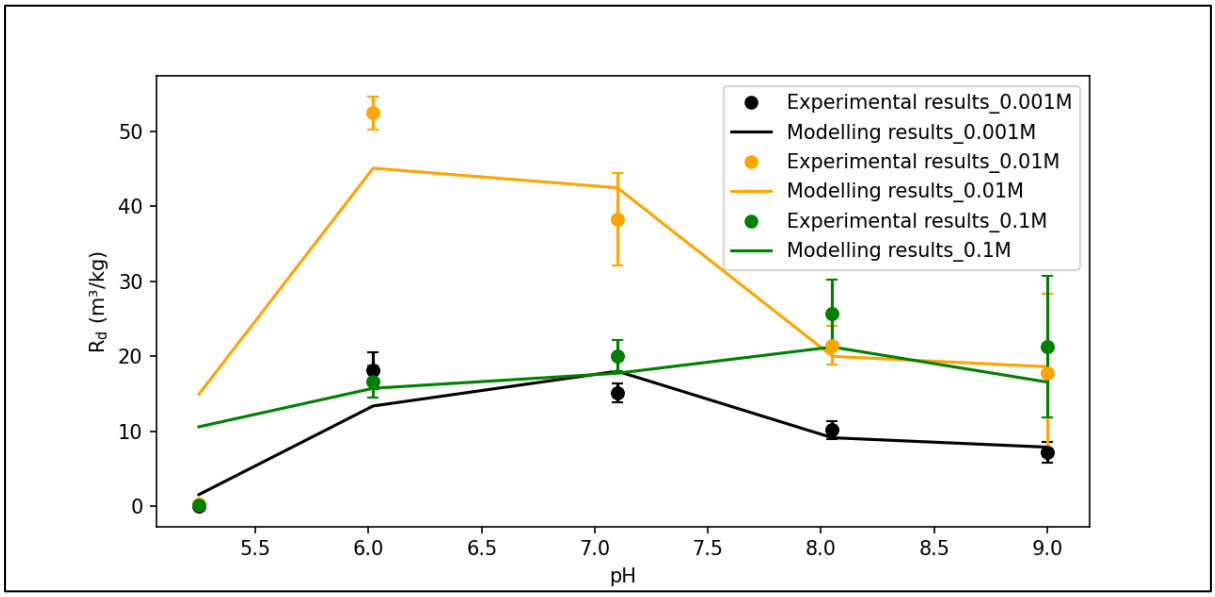

Figure 6. Experimental (points) and Modelling (line) for Am(III) sorption on biotite in 0.001 M, 0.01 M, and 0.1 M $NaClO_4$ solutions.

Figure 7 demonstrates that Am, similar to Eu, forms various hydrolysis products within the pH range of 5–9. Below pH 7.5, Eu^{3+} is the dominant species. However, at pH levels above 7.5, Eu^{3+} undergoes hydrolysis, resulting in the formation of $AmOH^{2+}$ and $Am(OH)_2^+$ aqueous species. Thus, in the pH range of 5–9 these species must be considered during the optimization process.

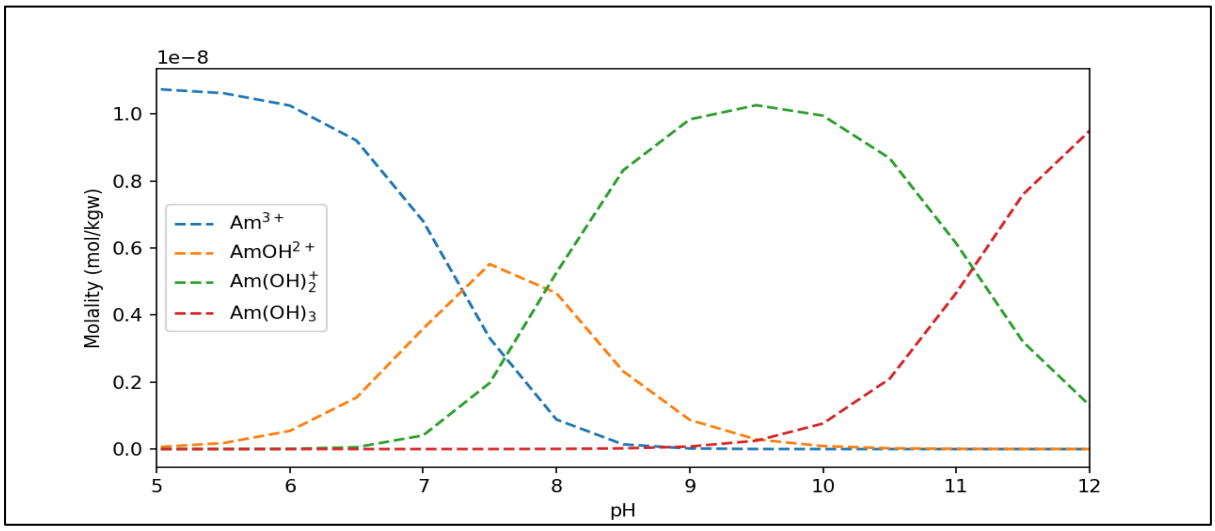

Figure 7. The aqueous speciation curve of Am as a function of pH

The Am sorption onto biotite was successfully modeled by accounting three surface complexation species: $\equiv SOAm^{2+}$,$\equiv SOAm(OH)^{+}$, $\equiv SOAm(OH)_2$, as well as one ion-

exchange species, AmX_3, across all three $NaClO_4$ concentrations (0.001 M, 0.01 M, and 0.1 M). Other potential species, such as $\equiv SOAm(OH)_3^-$ and $\equiv SOHAm^{3+}$ were found to contribute insignificantly to Am sorption and were therefore excluded from the model.

The model results, illustrated in Figure 8 (a, b, and c), indicate that at all ionic strengths (0.001 M, 0.01 M, and 0.1 M), Am sorption is primarily dominated by ion exchange (AmX_3) in the pH range ~6 to 7. At pH ~7, there was some contribution from the $\equiv SOAm^{2+}$ species was seen. However, at higher pH values (>8), Am sorption was mainly controlled by the hydroxylated species, $\equiv SOAm(OH)_2$ and $\equiv SOAm(OH)^+$. The reactions used in the model, along with the corresponding surface complexation and cation exchange constants, are provided in Table 4.

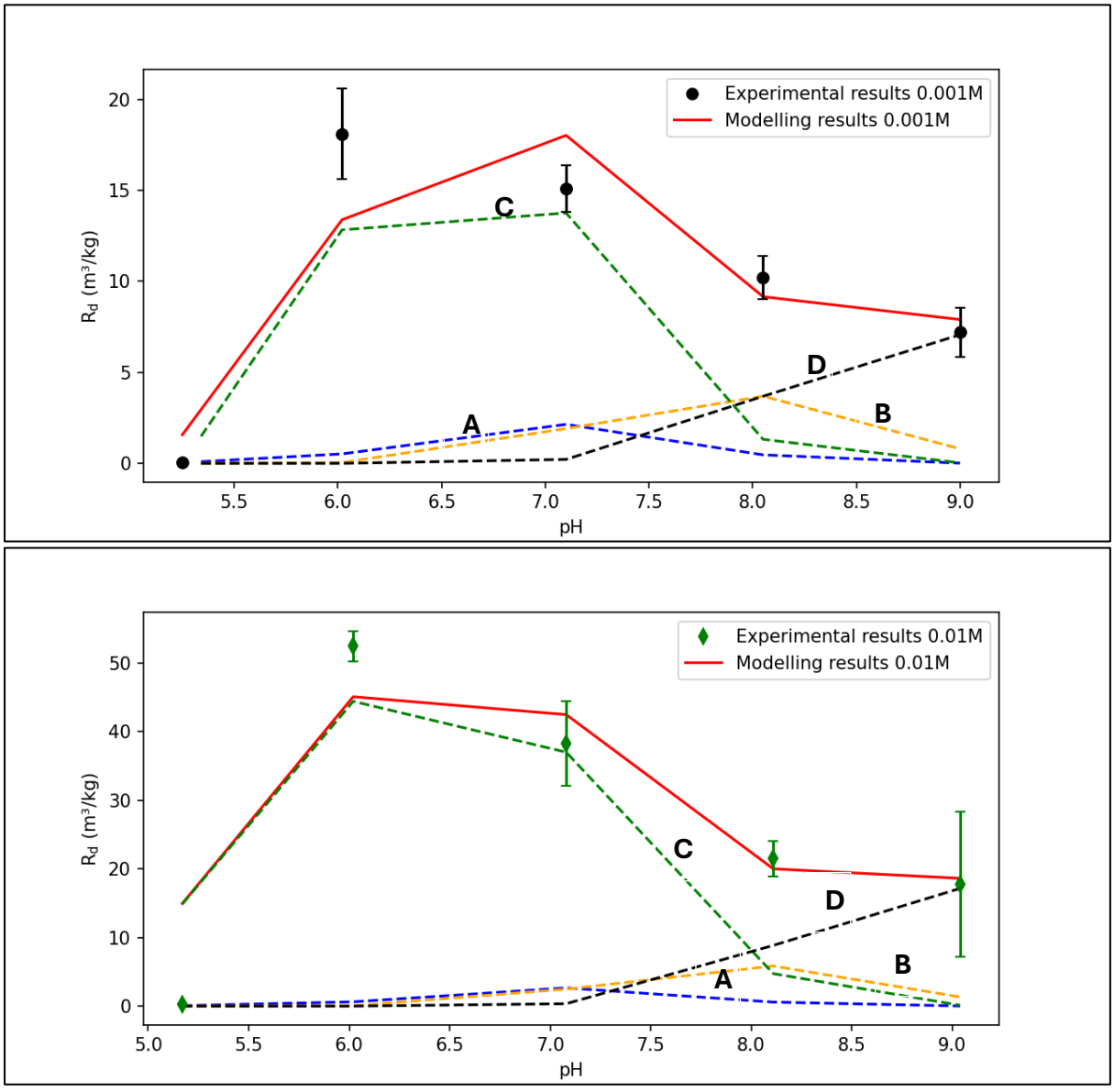

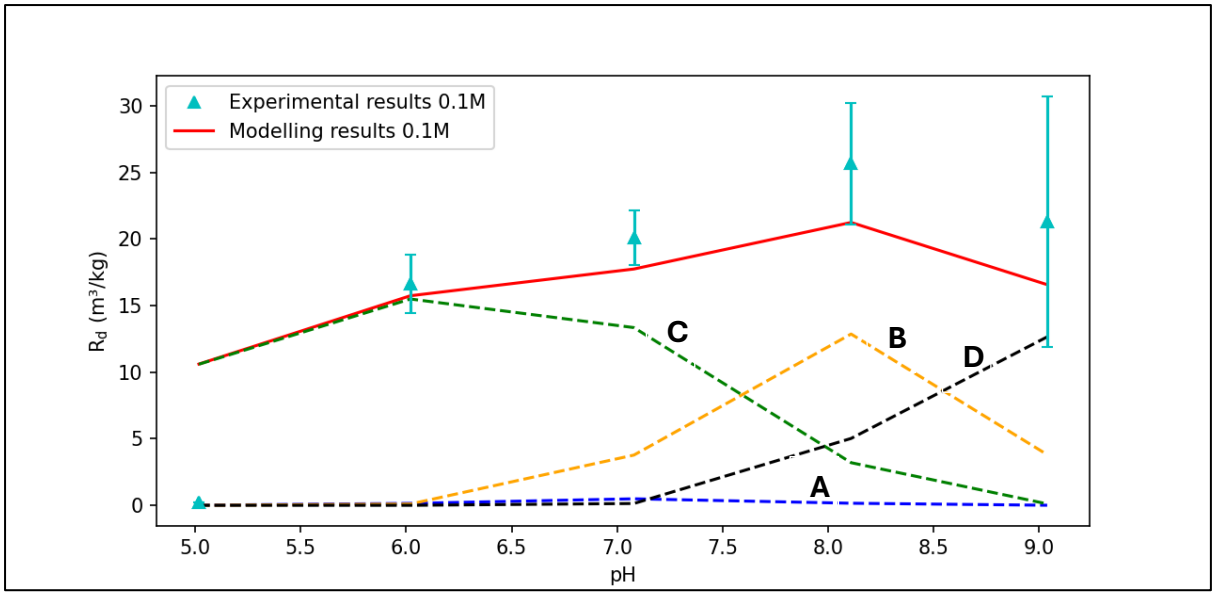

Figure 8. Am sorption experimental (symbol) and modelling (continuous line) results on biotite (a) 0.001 M, (b) 0.01 M and (c) 0.1 M $NaClO_4$ NaClO solution at 25 °C . The contribution of different Am(III) species in its sorption is represented by different curves: (A: blue line)≡ $SOAm,^{2+}$; (B: yellow line) ≡ $SOAm(OH)^{+}$; (C: green line) AmX_3; (D: black line). ≡ $SOAm(OH)_2$

Table 4: Surface complexation and cation exchange reactions and their associated constants at zero ionic strength (log_k°) for Am. Selectivity coefficients are for the specified ionic strength

Reactions	**log k° (25 °C)**
$\equiv SO^- + Am^{3+} \leftrightarrow \equiv SOAm^{2+}$	6.1 ± 0.2
$\equiv SO^- + Am(OH)^{2+} \leftrightarrow \equiv SOAm(OH)^{+}$	6.4 ± 0.7
$\equiv SO^- + Am(OH)_2^{+} \leftrightarrow \equiv SOAm(OH)_2$	6.2 ± 0.4
$\equiv SOH + Am^{3+} + 3H_2O \leftrightarrow \equiv SOAm(OH)_3^- + 4H^+$	Insignificant*
$\equiv SOH + Am^{3+} \leftrightarrow \equiv SOHAm^{3+}$	Insignificant*

Reaction/Ionic Strength at 25 °C	**0.001 M**	**0.01 M**	**0.1 M**
$Am^{3+} + 3NaX \leftrightarrow AmX3 + 3Na^+$	log_k = -2.4	log_k = 1.1	log_k = 4.0

*Inclusion of this species gave no improvement of error sum

5. Conclusions

The sorption of Ra and Am onto biotite was studied across three different background electrolyte concentrations (0.001M, 0.01M, and 0.1M) and a pH range of 5 to 9, under room temperature conditions in an inert nitrogen environment inside a glove box. Experimental results indicated that the sorption of both cations is strongly pH-dependent. However, Ra showed significant sensitivity to ionic strength, unlike Am, which exhibited no such dependency.

Comparing the R_d - values of Ra^{2+} and Am^{3+} with those of Ba^{2+} and Eu^{3+} from a previous study on Cs, Ba, Co, and Eu sorption onto biotite revealed a similar sorption trend between the cation pairs. However, Ra^{2+} and Am^{3+} exhibited distribution coefficients nearly two to three times higher than Ba^{2+} and Eu^{3+}, suggesting that using Ra^{2+} and Am^{3+} as analogs for Ba^{2+} and Eu^{3+} might underestimate the actual sorption of Ra and Am.

The sorption data for these two cations was successfully modeled using a 2-pKa, non-electrostatic, single-site type model. This model assumes one surface complexation site (presumably located on the biotite edges) and one cation exchange site (likely located on the mineral's basal plane).

The decrease in Ra sorption with increasing ionic strength, attributed to competition from H^+ and Na^+ ions, indicates that cation exchange is the dominant mechanism controlling Ra sorption, with surface complexation becoming significant at pH levels above 6. In contrast, for Am sorption, the model required a combination of surface complexation, including the sorption of hydrolyzed species, along with cation exchange to accurately capture its interaction with biotite.

The titration and batch sorption data were successfully modeled using the PHREEQC geochemical software, coupled with an optimization routine written in Python. This process yielded a distinct set of surface complexation constants and cation selectivity coefficients for both Ra and Am.

6. Acknowledgment

This research was supported by grants from SSM (Swedish Radiation Safety Authority). We thank Dr. A.M. Jakobsson for her valuable comments, which helped us improve the manuscript.

References

[1] A. Hedin and O. Olsson, "Crystalline rock as a repository for Swedish spent nuclear fuel," *Elements,* pp. 247-252, 2016.

[2] SKBF/KBS, “Kärnbränslecykelns slutsteg,” Svensk Kärnbränsleförsörjning AB (Swedish Nuclear Fuel and Waste Management Company), Stockholm, 1983.

[3] SKB, "Design and production of the KBS-3 repository (TR-10-12)," Svensk Kärnbränslehantering AB, Stockholm, 2010.

[4] SKB, "Long-term safety for the final repository for spent nuclear fuel at Forsmark Main report of the SR-Site project Volume III (TR-11-01)," Svensk Kärnbränslehantering AB, Stockholm, 2011.

[5] B. Miller and N. Marcos, "Process report - FEPs and scenarios for a spent fuel repository at Olkiluoto (Posiva Report 2007-12)," Posiva Oy, Olkiluoto, Finland, 2007.

[6] J. Crawford, "Bedrock Kd data and uncertainty assessment for application in SR-Site geosphere transport calculations (R-10-48)," Svensk Kärnbränslehantering AB, Stockholm, 2010.

[7] M. Hakanen, H. Ervanne and E. Puukko, "Safety case for the disposal of spent nuclear fuel at Olkiluoto - Radionuclide migration parameters for the geosphere (2012-41)," Posiva Oy, Olkiluoto, Finland, 2012.

[8] J. A. Davis, J. A. Coston, D. B. Kent and C. C. Fuller, "Application of the surface complexation concept to complex mineral assemblages," *Env. Sci. Technol.,* vol. 32, pp. 2820-2828, 1998.

[9] J. A. Davis, D. E. Meece, M. Kohler and G. P. Curtis, "Approaches to surface complexation modeling of uranium(VI) adsorption on aquifier sediments," *Geochim. Cosmochim. Acta,* vol. 68, pp. 3261-3641, 2004.

[10] H. Drake, B. Sandström and E.-L. Tullborg, "Mineralogy and geochemistry of rocks and fracture fillings from Forsmark and Oskarshamn: Compilation of data for SR-Can (R-06-109)," Svensk Kärnbränslehantering AB, Stockholm, 2006.

[11] E. Selnert, J. Byegård and H. Widestrand, "Forsmark site investigation - Laboratory measurements within the site investigation programme for the transprt properties of the rock, Final report (P-07-139)," Svensk Kärnbränslehantering AB, Stockholm, 2008.

[12] W. D. Nesse, Introduction to mineralogy, New York: Oxford University Press, 2000.

[13] R. M. Cornell, "Adsorption of cesium on minerals: A review," *J Radioanal. Nucl. Chem.,* vol. 171, pp. 483-500, 1993.

[14] S.-C. Tsai, T.-H. Wang, M.-H. Li, Y.-Y. Wei and S.-P. Teng, "Cesium adsorption and distribution onto crushed granite under different physicochemical conditions," *J. Hazard. Mat.,* vol. 161, pp. 854-861, 2009.

[15] K. Fukushi, Y. Hasegawa, K. Maeda, Y. Aoi, A. Tamura, S. Arai, Y. Yamamoto, D. Aosai and T. Mizuno, "Sorption of Eu(III) on granite: EPMA, LA-ICP-MS, batch and modeling studies," *Environ. Sci. Technol.,* vol. 47, pp. 12811-12818, 2013.

[16] Y. Tachi, T. Ebina, C. Takeda, T. Saito, H. Takahashi, Y. Ohuchi and A. J. Martin, "Matrix diffusion and sorption of Cs, Na, I and HTO in granodiorite: Laboratory-scale results and their extrapolation to the in situ conditions," *J. Contam. Hydrol.,* vol. 179, pp. 10-24, 2015.

[17] E. Muuri, J. Ikonen, M. Matara-aho, A. Lindberg, S. Holgersson, M. Voutilainen, M. Siitari-Kauppi and A. Martin, "Bahavior of Cs in Grimsel granodiorite: sorption on main minerals and crushed rock," *Radiochim. Acta,* vol. 104, pp. 575-582, 2016.

[18] K. L. Nagy, "Dissolution and precipitation kinetics of sheet silicates," *Rev. Mineral.,* vol. 31, pp. 173-225, 1995.

[19] J. P. McKinley, J. M. Zachara, S. M. Heald, A. Dohnalkova, M. G. Newville and S. R. Sutton, "Microscale distribution of cesium sorbed to Bbiotite and muscovite," *Environ. Sci. Technol.,* vol. 38, pp. 1017-1023, 2004.

[20] J. Kyllönen, M. Hakanen, A. Lindberg, R. Harjula, M. Vehkamäki and J. Lehto, "Modeling of cesium sorption on biotite using cation exchange selectivity coefficients," *Radiochim. Acta,* vol. 102, pp. 919-929, 2014.

[21] M. Söderlund, H. Ervänne, E. Muuri and J. Lehto, "The sorption of alkaline earth metals on biotite," *Geochem. J.,* vol. 53, pp. 223-234, 2019.

[22] S. Holgersson and P. Kumar, "A literature review on thermodynamic sorption models of radionuclides with some selected granitic minerals," *Front. Nucl. Eng.,* p. 1227170, 2023.

[23] T. E. Payne, V. Brendler, M. Ochs, B. Baeyens, P. L. Brown, J. A. Davis, C. Ekberg, D. A. Kulik, J. Luetzenkirchen, T. Missana, Y. Tachi, L. R. Van Loon and S. Altmann, "Guidelines for thermodynamic sorption modelling in the context of radioactive waste disposal," *Environ. Modell. Softw.,* vol. 42, pp. 143-156, 2013.

[24] E. Muuri, M. Matara-aho, E. Puhakka, J. Ikonen, A. Martin, L. Koskinen and M. Siitari-Kauppi, "The sorption and diffusion of 133Ba in crushed and intact granitic rocks from the Olkiluoto and Grimsel in-situ test sites," *Applied Geochemistry,* vol. 89, pp. 138-149, 2018.

[25] O. Fabritius, E. Puhakka, X. Li, A. Nurminen and M. Siitari-Kauppi, "Radium sorption on biotite; surface complexation modeling study," *Applied Geochemistry,* vol. 140, p. 105289, 2022.

[26] E. Puukko, M. Olin, E. Puhakka, M. Hakanen, A. Lindberg and J. Lehikoinen, "Sorption of nickel and europium on biotite," *In FUNMIG 3rd Annual Meeting,* pp. 265-272, 2007.

[27] S. Holgersson, H. Drake, A. Karlsson and L. Krall, "Biotite dissolution kinetics at pH 4 and 6.5 under anaerobic conditions and the release of dissolved Fe(II)," *Chem.Geol.,* vol. 662, p. 122204, 2024.

[28] I. Dubois, *Specific surface area of some minerals commonly found in granite,* Stockholm: Kungliga Tekniska Högskolan, 2011.

[29] S. Brunauer, P. H. Emmet and E. Teller, “Adsorption of gases in multimolecular layers,” *J. Am. Chem. Soc.,* vol. 60, pp. 309-319, 1938.

[30] Q. Yu, A. Kandegedara, Y. Xu and D. B. Rorabacher, “Avoiding interferences from Good´s buffers: a contiuous series of noncomplexing tertiary amine buffers covering the entire range of pH 3-11,” *Anal. Biochem.,* vol. 253, pp. 50-56, 1997.

[31] M. Andersson, H. Ervanne, M. A. Glaus, S. Holgersson, P. Karttunen, H. Laine, B. Lothenbach, I. Puigdomenech, B. Schwyn, M. Snellman, H. Ueda, M. Vuorio, E. Wieland and T. Yamamoto, "Development of methodology for evaluation of long-term safety aspects of organic cement paste components Working Report 2008-28," Posiva Oy, Olkiluoto, Finland, 2008.

[32] M. Bradbury and B. Baeyens, "Sorption modelling on illite Part I: Titration measurements and the sorption of Ni, Co, Eu and Sn," *Geochim. Cosmochim. Acta,* vol. 73, pp. 990-1003, 2009.

[33] M. Bradbury and B. Baeyens, "Sorption of Eu on Na-and Ca-montmorillonites: Experimental investigations and modelling with cation exchange and surface complexation," *Geochim. Cosmochim. Acta,* vol. 66, pp. 2325-2334, 2002.

[34] M. Söderlund, J. Virkanen, S. Holgersson and j. Lehto, "Sorption and speciation of selenium in boreal forest soil," *J. Environ. Radioact.,* vol. 164, pp. 220-231, 2016.

[35] X. Li, E. Puhakka, J. Ikonen, M. Söderlund, A. Lindberg, S. Holgersson, A. Martin and M. Siitari-Kauppi, "Sorption of Se species on mineral surfaces, part I: batch sorption and multi-site modelling," *Applied Geochemistry,* vol. 95, pp. 147-157, 2018.

[36] M. Rovira, J. Giménez, M. Martínez, X. Martínez-Lladó, J. de Pablo, V. Martí and L. Duro, "Sorption of selenium (IV) and selenium (VI) onto natural iron oxides: goethite and hematite," *J. Hazard. Mater.,* vol. 150, pp. 279-284, 2008.

[37] C. Ekberg and P. L. Brown, Hydrolysis of metal ions. Vol. 1 and 2., Wiley-VCH, 2016.

[38] D. L. Parkhurst and C. A. J. Appelo, *PHREEQC version 3: Computer Program for Speciation, Batch-Reaction, One-Dimensional Transport, and Inverse Geochemical Calculations,* U.S. Geological Survey, 2021.

[39] S. R. Charlton and D. L. Parkhurst, "Modules based on the geochemical model PHREEQC for use in scripting and programming languages," *Comput. Geosci.,* vol. 37, pp. 1653-1663, 2011.

[40] S. Rodriguez-Cruz and R. a. W. E. Jockusch, "Hydration energies and structures of alkaline earth metal ions, M2+ (H2O) n, n= 5− 7, M= Mg, Ca, Sr, and Ba," *Journal of the American Chemical Society,* vol. 121, pp. 8898-8906, 1999.

[41] B. Allard and G. a. K. T. Beall, "The sorption of actinides in igneous rocks," *Nuclear Technology,* pp. 474-480, 1980.

[42] S. Brunauer, P. H. Emmet and E. Teller, “Adsorption of gases in multimolecular layers,” *Journal of the American Chemical society,* vol. 60, pp. 309-319, 1938.

[43] E. Puukko, M. Olin, E. Puhakka, M. Hakanen, A. Lindberg and J. Lehikoinen, "Sorption of nickel and europium on biotite," Nuclear Decommisioning Authority, Moor Row, UK, 2007.

[44] J. Kyllönen, M. Hakanen, A. Lindberg, R. Harjula, M. Vehkamäki and . J. Lehto, "Modeling of cesium sorption on biotite using cation exchange selectivity coefficients," *Radiochim. Acta,* vol. 102, pp. 919-929, 2014.

[45] X. Li, E. Puhakka, L. Liu, W. Zhang, J. Ikonen, A. Lindberg and M. Siitari-Kauppi, "Multi-site surface complexation modelling of Se (IV) sorption on biotite," *Chemical Geology,* vol. 533, p. 119433, 2020.

[46] J. Luetzenkirchen, "Ionic strength effects on cation sorption to oxides: Macroscopic observations and their significance in microscopic interpretation," *J Colloid. Interface Sci.,* vol. 195, pp. 149-155, 1997.

[47] J. Luetzenkirchen, "Ionic strength effects on cation sorption to oxides: Macroscopic observations and their significance in microscopic interpretation," *J. Colloid. Interface Sci.,* vol. 195, pp. 149-155, 1997.

[48] B. Rotenberg, J.-P. Morel, V. Marry, P. Turq and N. Morel-Desrosiers, "On the driving force of cation exchange in clays: Insights from combined microcalorimetry experiments and molecular simulation," *Geochim. Cosmochim. Acta,* vol. 73, pp. 4034-4044, 2009.

[49] N. Jordan, T. Thoenen, K. Spahiu, J. Kelling, S. Starke and V. Brendler, "A critical review of the solution chemistry, solubility, and thermodynamics of europium: Recent advances on the Eu(III) hydrolysis," *Coordin. Chem. Rev.,* vol. 510, p. 215702, 2024.

[50] SKB, "Long-term safety for the final repository for spent nuclear fuel at Forsmark, Main report of the SR-Site project. Vol I-III (TR-11-01)," Svensk Kärnbränslehantering AB, Stockholm, 2011.

[51] J. Crawford, "Bedrock Kd data and uncertainty assessment for application in SR-Site geosphere transport calculations (R-10-48)," Svensk Kärnbränslehantering ABB, Stockholm, 2010.

[52] E. Muuri, J. Ikonen, M. Matara-aho, A. Lindberg, S. Holgersson, M. Voutilainen, M. Siitari-Kauppi and A. Martin, "Bahavior of Cs in Grimsel granodiorite: sorption on main minerals and crushed rock," *Radiochemica Acta,* vol. 104, pp. 575-582, 2016.

[53] S. Holgersson and P. Kumar, "A literature review on thermodynamic sorption models of radionuclides with some selected granitic minerals," *Front. Nucl. Eng.,* vol. 2, p. 1227170, 2023.

[54] J. Kyllönen, M. Hakanen, A. Lindberg, R. Harjula, M. Vehkamäki and J. Lehto, "Modeling of cesium sorption on biotite using cation exchange selectivity coefficients," *Radiochimica Acta,* vol. 102, pp. 919-929, 2014.

[55] M. Söderlund, H. Ervänne, E. Muuri and J. Lehto, "The sorption of alkaline earth metals on biotite," *Geochemical Journal,* vol. 53, pp. 223-234, 2019.

[56] M. H. Bradbury and B. Baeyens, "A generalized sorption model for the concentration dependent uptake of caesium by argillaceous rocks," *Journal of Contaminant Hydrology,* vol. 42, pp. 141-163, 2000.

[57] K. Furuya, K. Idemitsu, Y. Inagaki, T. Arima, T. Sasaki, Y. Kuroda, S. Uchikawa, S. Mitsugashira and Y. Suzuki, "Sorption of plutonium on a biotite mineral," Science Reports of the Research Institutes Tohoku University, Series A Physics, Tohoku, 1997.

[58] T. E. Payne, V. Brendler, M. Ochs, B. Baeyens, P. L. Brown, J. A. Davis, C. Ekberg, D. A. Kulik, J. Luetzenkirchen, T. Missana, Y. Tachi, L. R. Van Loon and S. Altmann, "Guidelines for thermodynamic sorption modelling in the context of radioactive waste disposal," *Environ. Modell. Softw.,* vol. 42, pp. 143-156, 2013.

[59] S. Holgersson, H. Drake, A. Karlsson and L. Krall, "Biotite dissolution kinetics at pH 4 and 6.5 under anaerobic conditions and the release of dissolved Fe(II)," *Chemical Geology,* vol. 662, p. 122204, 2024.

[60] G. Gran, "Determination of the equivalent point in potentiometric titrations," *Acta Chem. Scand.,* vol. 4, pp. 557-559, 1950.

[61] A.-M. Jakobsson, *Measurement and modelling using surface complexation of cation (II to VI) sorption onto mineral oxides,* Göteborg: Chalmers University of Technology, Department of Nuclear Chemistry, 1999.

[62] Q. Yu, A. Kandegedara, Y. Xu and D. B. Rorabacher, “Avoiding interferences from Good´s buffers: a contiuous series of noncomplexing tertiary amine buffers covering the entire range of pH 3-11,” *Anal. Biochem.,* vol. 253, pp. 50-56, 1997.

[63] M. Andersson, H. Ervanne, M. A. Glaus, S. Holgersson, P. Karttunen, H. Laine, B. Lothenbach, I. Puigdomenech, B. Schwyn, M. Snellman, H. Ueda, M. Vuorio, E. Wieland and T. Yamamoto, "Development of methodology for evaluation of long-term safety aspects of organic cement paste components," POSIVA, Olkiluoto, 2008.

[64] A. W. Bray, E. H. Oelkers, S. Bonneville, D. Wolff-Boenisch, N. J. Potts, G. Fones and L. G. Benning, “Effect of pH, grain size, and organic ligands on biotite weathering rates,” *Geochim. Cosmochim. Acta,* vol. 164, pp. 127-145, 2015.

[65] S. Brunauer, P. H. Emmet and E. Teller, “Adsorption of gases in multimolecular layers,” *J. Am. Chem. Soc.,* vol. 60, pp. 309-319, 1938.

[66] L. Wissmeier and D. A. Barry, "Simulation tool for variably saturated flow with comprehensive geochemical raction in the two and three dimensional domains," *Env.Modell.Softw.,* vol. 26, pp. 210-218, 2011.

[67] X. Li, E. Puhakka, L. Liu, W. Zhang, J. Ikonen, A. Lindberg and M. Siitari-Kauppi, "Multi-site surface complexation modelling of Se(IV) sorption on biotite," *Chem. Geol.,* vol. 533, 2020.

[68] C. Schollenberger and R. Simon, "Determination of exchange capacity and exchangeable bases in soil—ammonium acetate method," *Soil Sci.,* vol. 59, pp. 13-24, 1945.

[69] Y. G. Berubé, G. Y. Onoda and P. L. De Bruyn, "Proton adsorption at the ferric oxide/aqueous solution interface," *Surface Science,* vol. 8, pp. 448-461, 1967.

[70] A. Jakobsson, Y. Albinsson and R. Rundberg, "Studies of surface complexation of H+ , NpO2+, Co2+, Th4+ onto TiO2 and H+, UO22+ onto alumina (TR-98-15)," Svensk Kärnbränslehantering AB, Stockholm, 1998.

[71] Å. Zazzi, A. Jakobsson and S. Wold, "Ni (II) sorption on natural chlorite," *Appl. Geochem.,* vol. 27, pp. 1189-1193, 2012.

[72] A. W. Bray, L. G. Benning, S. Bonneville and E. H. Oelkers, "Biotite surface chemistry as a function of aqueous fluid composition," *Geochi. Cosmochim. Acta,* vol. 128, pp. 58-70, 2014.

[73] J. Crank, The Mathematics of diffusion, 2nd ed., New York: Oxford University Press, 1979.

[74] A. W. Bray, E. H. Oelkers, S. Bonneville, D. Wolff-Boenisch, N. J. Potts, G. Fones and L. G. Benning, "The effect of pH, grain size and organic ligands on biotite weathering rates," *Geochimica et Cosmochimica Acta,* vol. 164, pp. 127-145, 2015.

[75] M. Kosmulski, "The pH dependent surface charging and points of zero charge. VIII Update.," *Adv.Colloid Interface Sc.,* p. 102064, 2020.

[76] F. Macht, K. Eusterhues, G. J. Pronk and K. U. Totsche, "Specific surface area of clay minerals: Comparison between atomic force microscopy meaurements and bulk.gas (N2) and -liquid (EGME) adsorption methods," *App. Clay. Sci.,* pp. 20-26, 2011.

[77] W. Stumm and J. J. Morgan, Aquatic Chemistry, 3rd Ed., New York: Wiley, 1996.

[78] E. Muuri, M. Siitari-Kauppi, M. Matara-aho, J. Ikonen, A. Lindberg, L. Qian and L. Koskinen, "Cesium sorption and diffusion on crystalline rock: Olkiluoto casestudy," *Journal of Radioanalytical and Nuclear Chemistry,* vol. 311, pp. 439-446, 2017.

[79] S. Holgersson, "Studies on batch sorption methodologies: Eu sorption onto Kivetty granite," *Procedia Chemistry,* vol. 7, pp. 629-640, 2012.

[80] P. Kumar, S. Holgersson and C. Ekberg, "Sorption of Cs, Ba, Co and Eu onto biotite at 40 and 60 C - a combined experimental and modelling study," *J. Contamin. Hydrol.,* in press.

[81] R. .. Hunter, 1989.

[82] M. Eveliina, I. Jussi, M. Minja, L. Antero, H. Stellan, V. Mikko, S. Marja and A. Martin, "Behavior of Cs in Grimsel granodiorite: sorption on main minerals and crushed rock," *Radiochim. Acta,* vol. 104, pp. 575-582, 2016.